Journal of Neuro-Oncology (2006) 78: 145–151
DOI 10.1007/s11060-005-9069-x

Clinical–patient studies

PET Imaging of cerebral astrocytoma with ^{13}N-ammonia

Zhang Xiangsong[1,2], Liang Changhong[3], Chen Weian[1] and Zhou Dong[4]
[1]*Department of Nuclear Medicine, The First Affiliated Hospital, Sun Yat-sen University, Guangzhou, China;* [2]*Department of Nuclear Medicine, Guangdong Provincial People's Hospital, Guangzhou, China;* [3]*Department of Radiology, Guangdong Provincial People's Hospital, Guangzhou, China;* [4]*Department of Neurosurgery, Guangdong Provincial People's Hospital, Guangzhou, China*

Key words: astrocytoma, ammonia, nitrogen radioisotopes, PET

Summary

We performed this study in order to assess the clinical potential of ^{13}N-ammonia PET in patients with cerebral astrocytoma.

Methods: Dynamic ^{13}N-ammonia PET was performed in 25 patients with suspected cerebral gliomas or recurrent cerebral astrocytomas (19 male and 6 female patients; age range 18–64 years) detected by MRI. The histopathological diagnoses were made for all cases either by biopsy or craniotomy, except for one patient with brain infarction and one patient with brain radiation necrosis confirmed by repeated MRI imaging. PET images were visually inspected, and the tumor-to-white matter count (T/W) ratios and the perfusion index (PI) of the tumors were determined.

Results: Six out of nine cases of low-grade gliomas were detected with ^{13}N-ammonia PET, and three non-astrocytoma low-grade gliomas were not detected with ^{13}N-ammonia PET. All 11 high-grade astrocytomas exhibited markedly increased uptake of ^{13}N-ammonia. The five non-neoplastic lesions exhibited low uptake, low T/W ratios and low PI. The significant differences were observed between high-grade and low-grade gliomas with respect to both the T/W ratios and PI (T/W ratios: 5.92 ± 2.27, $n = 11$ vs. 1.66 ± 0.61, $n = 9$, $P < 0.01$; PI: 5.22 ± 1.67, $n = 11$ vs. 1.60 ± 0.54, $n = 9$, $P < 0.01$). There were the significant differences between the T/W ratios and PI in low-grade astrocytomas and that in non-neoplastic lesions (T/W ratios: 2.00 ± 0.42, $n = 6$ vs. 0.97 ± 0.11, $n = 5$, $P < 0.01$; PI: 1.89 ± 0.37, $n = 6$ vs. 0.99 ± 0.03, $n = 5$, $P < 0.01$).

Conclusions: There is a substantial uptake of ^{13}N-ammonia in cerebral astrocytomas. ^{13}N-ammonia PET may enable differentiation between low- and high-grade astrocytomas, and has the potential to enable differentiation between low-grade astrocytomas and non-neoplastic lesions.

Introduction

Gliomas constitute approximately 45% of all brain tumors, and low-grade gliomas constitute approximately 15% of all brain tumors. Gliomas are typically subdivided in astrocytic tumors, oligodendroglial tumors, ependymal tumors, and mixed gliomas. Astrocytic tumors are further graded into grade Ito grade IV according to specific pathologic criteria that include cellular atypia, mitotic activity, necrosis, endothelial proliferation, etc.

CT and MRI with contrast are excellent tools for tumor localization. These methods are however often unable to characterize the underlying histopathology. Particular areas of difficulty include defining tumor extension and grade, as well as differentiating tumor recurrence from necrosis or scar [1].

^{18}F-FDG is now widely used in PET scanning to evaluate various tumors. ^{18}F-FDG PET offer considerably improved diagnosis of cerebral gliomas as compared with conventional radiological methods, but the fact that some low-grade gliomas show hypo- or isometabolism compared with normal brain tissue on FDG PET has caused problems in the detection of primary or recurrent tumors and in the differentiation from benign lesions. Amino-acid tracers, such as ^{11}C-methyl-methionine (MET), perform better for this purpose and thus play a complementary role to FDG [2]. These benefits are offset by a potentially lower specificity of MET for tumor tissues. The uptake is partly related to passive diffusion in tumors with significant breakdown of the blood–brain barrier (BBB) and this may limit the specificity of MET in diagnosing recurrence in areas of high contrast enhancement on CT or MRI [3]. Ogawa et al. studied 50 glioma patients with MET PET. They observed MET uptake in only approximately 60% of low-grade tumors [4]. ^{11}C-chonine PET has the potential to enable differentiation between low-grade and high-grade gliomas, but not to differentiate low-grade gliomas from non-neoplastic lesions [5].

In this study we investigated whether there was uptake of ^{13}N-ammonia in cerebral astrocytomas, and preliminarily assessed the clinical potential of ^{13}N-ammonia PET in patients with cerebral astrocytoma.

Material and methods

Patients

Twenty-five patients with suspected cerebral gliomas or recurrent cerebral astrocytomas (19 male and 6 female patients; age range 18–64 years) were selected. T2-weighted and gadolinium-enhanced T1-weighted MR images were available for all patients. The exact histopathological diagnoses were proven in all cases either by biopsy or craniotomy performed within 1–2 weeks after PET scanning, based on the classification of the World Health Organization (WHO) [6], except for one patient with brain infarction and one patient with brain radiation necrosis confirmed by repeated MRI imaging.

The study was approved by the hospital ethics committee and each individual participating in the study gave his or her informed consent.

PET and MR imaging

Dynamic PET was performed as a 3-dimensional acquisition on an ECAT HR$^+$ scanner (Siemens/CTI) with a 5-min transmission scan. The trans-axial spatial resolution was 4.2 mm full-width at half-maximum (FWHM) at center of the field of view. The emission protocol was a 19-min dynamic scan (10 s×12, 30 s×4, and 900 s×1) triggered simultaneously with a bolus injection of 444–592 MBq of ^{13}N-ammonia.

All MR imaging examinations were performed with the clinical 1.5-T imaging units. Non-enhanced axial T1-weighted and T2-weighted images were performed. T1-weighted gadiolinium-enhanced MR images were obtained after administration of 0.1 mmol/kg gadopentetate dimeglumine.

Preparation of ^{13}N-ammonia

^{13}N was prepared by the ^{16}O (p, α)^{13}N nuclear reaction in a water target with the RDS-111 cyclotron (CTI). The target water was added to a reaction vessel containing Devarda's alloy and NaOH pellets to reduce oxides of ^{13}N to ammonia gas. The ^{13}N-ammonia was trapped in physiological saline acidified by adding 0.1 N HCl. Prior to delivery to the patient area, the solution was neutralized with 0.1 N NaOH and passed through a Millipore filter. The radiochemical purity of ^{13}N-ammonia was greater than 99%.

Data analysis

Attenuation-corrected images obtained with ^{13}N-ammonia were reconstructed using an ordered subset-expectation maximization (OS-EM) algorithm with 128×128 matrix.

All PET images were interpreted by two experienced nuclear physicians. Based on comparison with the surrounding background radioactivity, lesion uptake was classified into one of four categories: no uptake, faint uptake, moderate uptake or intense uptake. Moderate

Table 1. Patients' characteristics

Case No.	Age	Sex	Diagnosis	Site of disease	Visu.	T/W	PI
Low-grade gliomas							
1	52	M	Diffuse astrocytoma	Rt. hippocampus	+	2.76	2.56
2	46	F	Diffuse astrocytoma	Lt. hippocampus	+	1.86	1.78
3	21	M	Fibrillary astrocytoma	Lt. temporal	+	1.55	1.42
4	45	F	Fibrillary astrocytoma	Lt. temporal	+	2.17	1.94
5	26	M	Fibrillary astrocytoma	Rt. temporal	+	1.92	1.85
6	37	M	Gemstocytic astrocytoma	Lt. parietal & occipital	+	1.75	1.82
7	55	M	Oligodendroglioma	Lt. temporal & occipital	–	1.03	1.01
8	25	M	Oligodendroglioma	Rt. temporal	–	0.93	1.02
9	18	F	DNT	Rt. parietal	–	0.98	0.97
High-grade Gliomas							
10	62	M	Anaplastic astrocytoma	Rt. occipital	+	9.75	7.15
11	37	M	Anaplastic astrocytoma	Lt. Frontal	+	4.28	4.45
12	36	M	Anaplastic astrocytoma	Rt. occipital	+	3.36	3.02
13	38	M	Anaplastic astrocytoma	Lt. temporal	+	6.48	5.92
14	20	M	Anaplastic astrocytoma	Rt. frontal	+	6.30	6.31
15	45	M	Glioblastoma	Rt. frontal	+	3.26	3.15
16	27	M	Glioblastoma	Lt. & Rt. frontal	+	4.14	3.91
17	50	M	Glioblastoma	Rt. temporal	+	8.60	6.53
18	53	M	Glioblastoma	Lt. parietal	+	7.21	6.80
19	54	F	Glioblastoma	Lt. temporal	+	3.89	3.26
20	32	F	Glioblastoma	Rt. occipital	+	7.85	6.97
Non-neoplastic lesions							
21	38	M	Radiation necrosis	Rt. temporal	–	0.85	0.94
22	22	F	Radiation necrosis	Rt. Occipital	–	0.90	0.98
23	64	M	Brain infarction	Lt. frontal	–	0.93	1.01
24	28	M	Encephalitis	Rt. Occipital	–	1.12	1.03
25	46	M	Encephalitis	Lt. frontal	–	1.03	0.99

DNT – Dysembryoplastic neuroepithelial tumor, Lt. – left, Rt. – right, Visu. – visual result.

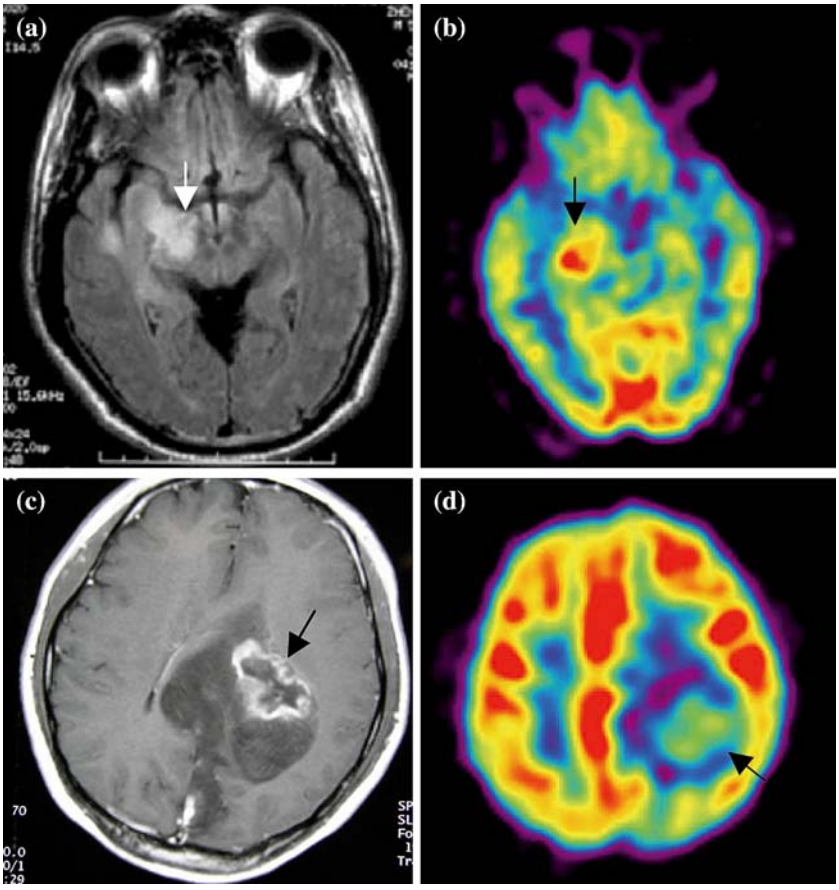

Figure 1. (a, b) A 52-year-old male with diffuse astrocytoma. (a) Fluid-attenuated inversion-recovery (FLAIR) MR imaging shows a high signal area in the right hippocampus. (b) A ^{13}N-ammonia PET image obtained at 4 min after injection demonstrates increased tumor uptake of ^{13}N-ammonia. (c, d) A 37-year-old male with gemstocytic astrocytoma. (c) T1-weighted gadiolinium-enhanced MR imaging shows an enhanced lesion with surrouding edema in the left parietal and occipital lobe. (d) A ^{13}N-ammonia PET image obtained at 4 min after injection demonstrates increased tumor uptake of ^{13}N-ammonia.

and intense uptake was defined as positive results of visual interpretation (+), and faint and no uptake was defined as negative results (−).

Regions of interest (ROIs) 10 mm in diameter were outlined on the site of maximum ^{13}N-ammonia tumor uptake and the contralateral white matter in the trans-axial planes across the dynamic PET frames. Counts per pixel in the tumors and white matters were calculated from the ROIs. The tumor-to-white matter (T/W) count ratios were determined on the last PET frame, and the average count ratios of tumor-to-white matter on the first 12 PET frames were calculated as the perfusion index (PI) of the tumors.

Statistic analysis

Differences in the T/W and PI were examined among tumors of different histological grade and non-neoplastic lesions. Statistic significance was determined using the Mann–Whitney test. A probability of <0.01 was considered significant.

Results

Patients' characteristics, including age, gender, histopathological features, tumor localization, ^{13}N-ammonia PET visual results, PI and T/W ratios are presented in Table 1.

Six out of nine cases of low-grade gliomas (WHO grade I or II) were detected with ^{13}N-ammonia PET (Figure 1), and three non-astrocytoma low-grade gliomas were not detected with ^{13}N-ammonia PET (Figure 2). The T/W ratios in low-grade gliomas ranged from 0.93 to 2.76, with a mean of 1.66 ± 0.61 ($n=9$), PI ranged from 0.97 to 2.56, with a mean of 1.60 ± 0.54 ($n=9$). All 11 high-grade astrocytomas (WHO grade I or II) exhibited markedly increased uptake of ^{13}N-ammonia (Figure 3), and the T/W ratios in high-grade astrocytomas ranged from 3.26 to 9.75, with a mean of 5.92 ± 2.27 ($n=11$), PI ranged from 3.02 to 7.15, with a mean of 5.22 ± 1.67 ($n=11$).

The five non-neoplastic lesions, two encephalitis, two radiation necrosis and one brain infarction, exhibited low uptake, low T/W ratios and low PI (Figure 4), and the T/W ratios in non-neoplastic lesions ranged from 0.85 to 1.12, with a mean of 0.97 ± 0.11 ($n=5$), PI ranged from 0.94 to 1.03, with a mean of 0.99 ± 0.03 ($n=5$).

The typical dynamic ^{13}N-ammonia PET images of low-grade astrocytoma, high-grade astrocytoma and non-neoplastic lesion are demonstrated in Figure 5, showing that the radioactivity in the high-grade astrocytomas

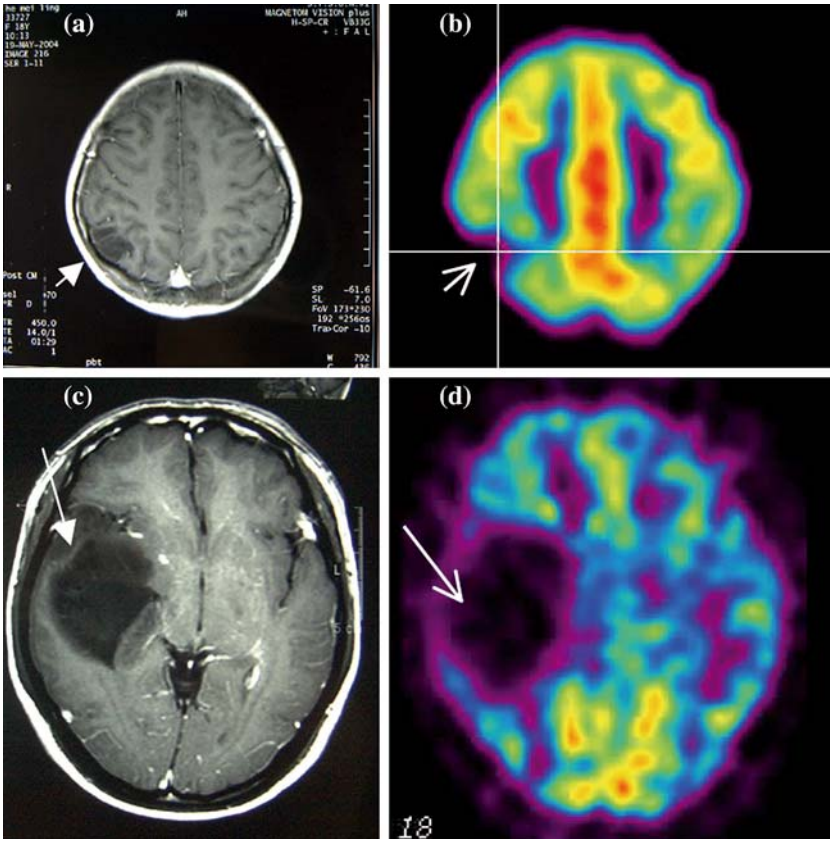

Figure 2. (a, b) An 18-year-old female with DNT. (b) T1-weighted MR imaging shows a low signal area in the right parietal lobe. (b) A ^{13}N-ammonia PET image obtained at 4 min after injection demonstrates decreased tumor uptake of ^{13}N-ammonia. (c, d) A 25-year-old male with oligodendroglioma. (c) T1-weighted gadiolinium-enhanced MR imaging shows a non-enhanced lesion in the right temporal lobe. (d) A ^{13}N-ammonia PET image obtained at 4 min after injection demonstrates decreased tumor uptake of ^{13}N-ammonia.

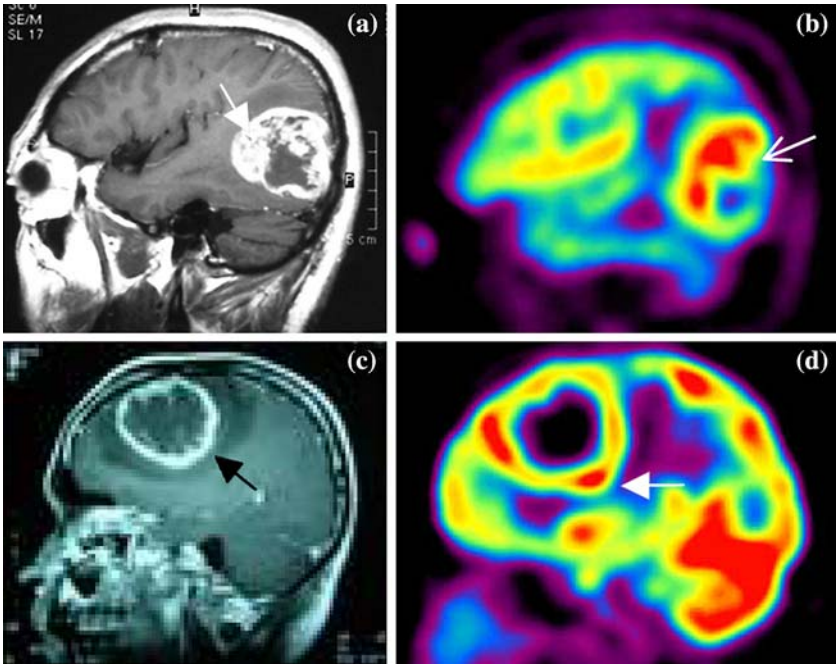

Figure 3. (a, b) A 62-year-old male with anaplastic astrocytoma. (a) T1-weighted gadiolinium-enhanced MR imaging shows a ring-like enhanced lesion in the right occipital lobe. (b) A ^{13}N-ammonia PET image obtained at 4 min after injection demonstrates increased uptake of ^{13}N-ammonia in the tumor margin and decreased uptake of ^{13}N-ammonia in the tumor center. (**c,** d) A 45-year-old male with glioblastoma. (c) T1-weighted gadiolinium-enhanced MR imaging shows a ring-like enhanced lesion in the right frontal lobe. (d) A ^{13}N-ammonia PET image obtained at 4 min after injection demonstrates increased uptake of ^{13}N-ammonia in the tumor margin and decreased uptake of ^{13}N-ammonia in the tumor center.

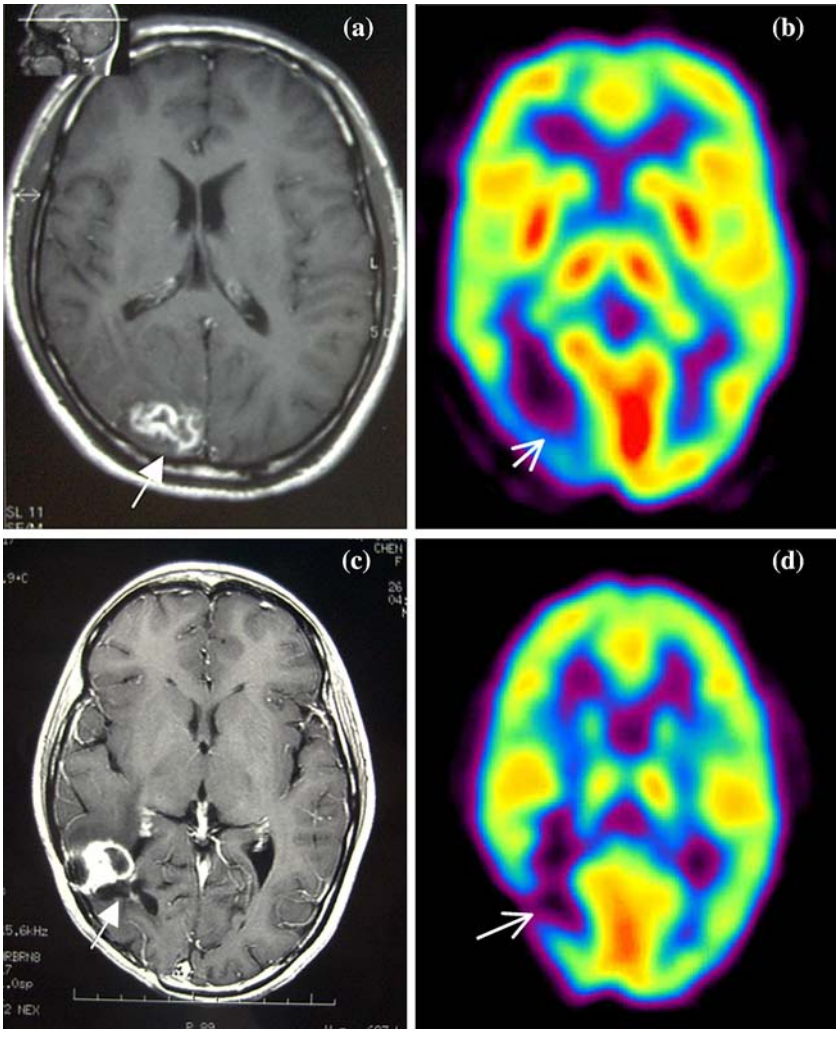

Figure 4. (a, b) A 28-year-old male with chronic encephalitis. (a) T1-weighted gadiolinium-enhanced MR imaging shows an enhanced lesion in the right occipital lobe. (b) A ^{13}N-ammonia PET image obtained at 4 min after injection demonstrates decreased lesion uptake of ^{13}N-ammonia. (c, d) A 22-year-old female with radiation necrosis two years after surgery and radiotherapy for glioblastoma. (c) T1-weighted gadiolinium-enhanced MR imaging shows a ring-like enhanced lesion in the right occipital lobe. (d) A ^{13}N-ammonia PET image obtained at 4 min after injection demonstrates decreased lesion uptake of ^{13}N-ammonia.

begin to markedly exceed surrounding brain radioactivity immediately after injection, in the low-grade astrocytomas begin to moderately exceed surrounding brain radioactivity approximately 1 min after injection, whereas the radioactivity in the non-neoplastic lesions were always lower than surrounding brain radioactivity after injection.

The significant differences were observed between high-grade and low-grade gliomas with respect to both the T/W ratios and PI (T/W ratios: 5.92 ± 2.27, $n = 11$ vs. 1.66 ± 0.61, $n = 9$, $P < 0.01$; PI: 5.22 ± 1.67, $n = 11$ vs. 1.60 ± 0.54, $n = 9$, $P < 0.01$). There were the significant differences between the T/W ratios and PI in low-grade astrocytomas and that in non-neoplastic lesions (T/W ratios: 2.00 ± 0.42, $n = 6$ vs. 0.97 ± 0.11, $n = 5$, $P < 0.01$; PI:1.89 ± 0.37, $n = 6$ vs. 0.99 ± 0.03, $n = 5$, $P < 0.01$). However, no significant differences were found between non-neoplastic lesions and non-astrocytic low-grade gliomas (T/W ratios: 0.97 ± 0.11, $n = 5$ vs. 0.98 ± 0.05, $n = 3$, $P > 0.01$; PI: 0.99 ± 0.03, $n = 5$ vs. 1.0 ± 0.03, $n = 3$, $P > 0.01$).

Discussion

MRI with contrast is an excellent tool for the detection and location of brain tumors, whereas PET scanning provides important information on a tumor's degree of malignancy. Thus PET scanning provides prognostic information and can detect tumor recurrence after treatment. We performed this study in order to assess the clinical potential of ^{13}N-ammonia PET in patients with cerebral astrocytomas.

We found the increased ^{13}N-ammonia uptake in all 11 high-grade astrocytomas and 6 low-grade astrocytomas, whereas three non-astrocytoma low-grade gliomas and five non-neoplastic lesions showed the decreased ^{13}N-ammonia uptake. These findings suggest that ^{13}N-ammonia PET can be useful in the detection of cerebral astrocytoma, and has the potential to enable differentiation between low-grade astrocytomas and non-neoplastic lesions. PI and T/W count ratios of tumors obtained with dynamic ^{13}N-ammonia PET in high-grade astrocytomas were significantly higher than those in

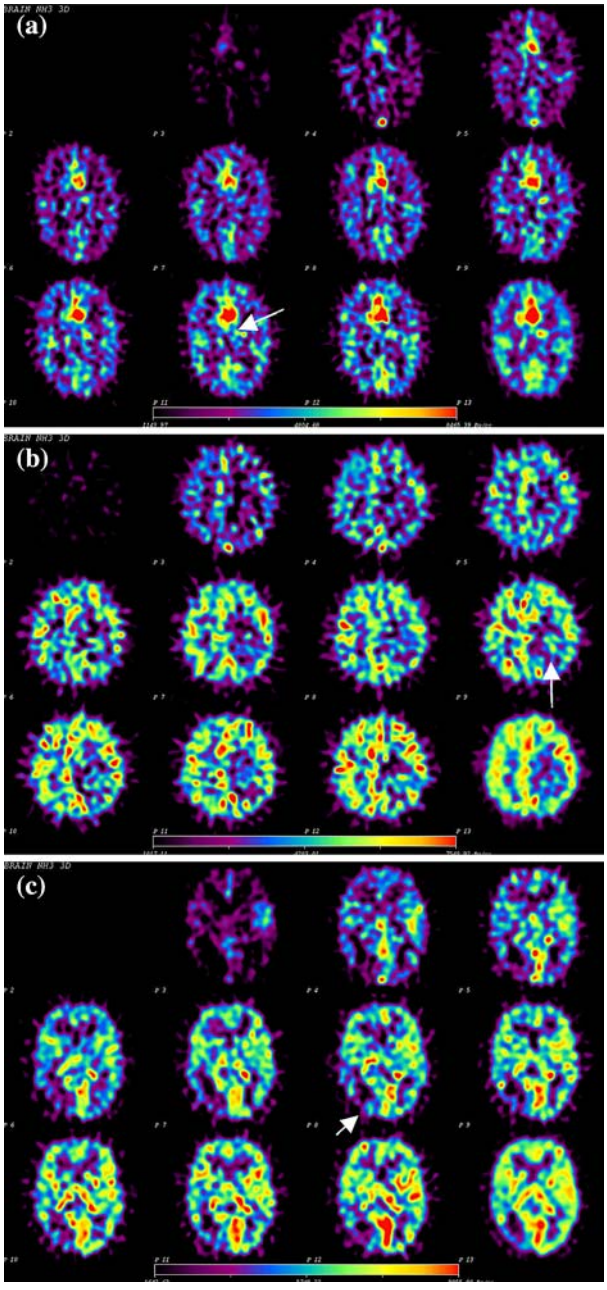

Figure 5. Dynamic PET images were obtained simultaneously after a bolus injection of ^{13}N-ammonia with 10 s for each image. (a) A 37-year-old male with anaplastic astrocytoma in the right frontal lobe. The PET images show the radioactivity in the tumor beginning to markedly exceed surrounding brain radioactivity immediately after injection. (b) A 37-year-old female with gemstocytic astrocytoma in the left parietal lobe. The PET images show the radioactivity in the tumor beginning to moderately exceed surrounding brain radioactivity approximately 1 min after injection. (c) A 28-year-old male with chronic encephalitis in the right occipital lobe. The PET images show the radioactivity in the lesion being always lower than surrounding brain radioactivity after injection.

low-grade gliomas. This finding suggests ^{13}N-ammonia uptake in astrocytomas may be related to the histological tumor grade. Moreover, the degree of tumor uptake of ^{13}N-ammonia might enable differentiation between low-grade and high-grade astrocyomas. However, the number of cases is small to definitely say that there is not a true difference between non-neoplastic lesions and non-astrocytic low-grade gliomas.

Our results were different from other studies reported before. Hoop et al. observed one recurrent astrocytoma and one glioma showed reduced uptake of ^{13}N-ammonia at the lesions [7]. Schelstraete et al. observed little or no extra uptake of ^{13}N-ammonia in four primary brain tumors [8]. Benard et al. thought ^{13}N-ammonia was unsuccessful in visualizing primary brain tumors [9]. These studies were done in 1976 and 1982, and the spatial resolution of the PET scanner used in Schelstraete's study was poor with 13 ± 1 mm FWHM. The number of patients was small, and the exact histopathological diagnoses were not given.

^{13}N-ammonia has been proved to be a good indicator of myocardial blood flow [10]. Phelps et al. [11] using PET with normal volunteers showed that the relative ^{13}N concentrations in structures of the brain were in good agreement with the relative capillary densities and/or cerebral blood flow (CBF). The net ^{13}N-ammonia extraction of brain tissues subsequent to an i.v. injection increases non-linearly with CBF, and depends primarily upon CBF, capillary permeability-surface product (PS) and integrity of the glutamate-glutamine synthetase reaction [12].

In analogy with what is known about ^{13}N-ammonia uptake in myocardium and brain, one may assume that the uptake of ^{13}N-ammonia in brain tumors is probably governed by two main factors: the capillary blood flow in the tumor and the metabolic properties of the tumor. Another factor should be considered that cerebral gliomas exhibit blood–brain barrier (BBB) disruption, and BBB permeability increases, especially, in high-grade gliomas.

Uptake of ^{13}N-ammonia by the myocardium has been shown to depend greatly upon the availability of the enzyme glutamine synthetase, and to be markedly reduced whenever the glutamine synthetase inhibitor methionine-sulphoximine (MSO) is administrated [13]. The glutamine synthetase (GS) reaction is the major route for metabolic trapping of ^{13}N-ammonia in brain tissues, and the conversion of ammonia to glutamine in brain is exceedingly rapid [14]. Pilkington et al. [15] found all astrocytomas showed positive staining with GS using the indirect immunoperoxidase and peroxidase-anti-peroxidase methods, the degree of which was related to the extent of differentiation and the amount of cytoplasm of the constituent cells. Ependymomas were only weakly positive, and Oligodendrocytomas and meningiomas were generally negative apart from occasional astrocytes within the former neoplasms. McCormick et al. and Akimoto also observed the similar results [16,17]. These findings suggest ^{13}N-ammonia may be metabolically trapped within the astrocytomas via the glutamate–glutamine pathway. The future studies of PET and GS staining would be important to explain the different accumulation of ^{13}N-ammonia in astrocytic and oligodendroglial tumors.

The malignant brain tumors are highly vascular. However, tumor circulation in situ are influenced by such factors as arterial blood pressure, blood gas, and intracranial pressure reflecting mass effect of the tumor or obstruction of cerebrospinal fluid pathways. Tumor vessels lacking autoregulation are more susceptible to

such factors and may result in variety of responses. Mineura et al. [18] found high-grade gliomas did not show significant increases in rCBF obtained with $C^{15}O_2$ PET. However, in our study ^{13}N-ammonia uptake in high-grade astrocytomas were significantly higher than those in low-grade gliomas and in non-neoplastic lesions.

In vivo proton magnetic resonance spectroscopy (MRS) provides a noninvasive method of examining a wide variety of cerebral metabolites in both healthy subjects and patients with various brain diseases. Pruel et al. [19] correctly classified 104 of 105 MR spectra of five kinds of brain tumors and the normal brain tissues by linear discriminant analysis using multi-voxel spectroscopy. MRS was proved to be useful in determining if lesions are low- or high-grade and differentiating recurrent or residual brain tumor from cerebral necrosis [20,21]. However, these metabolic characteristics exhibited large variations within each subtype of glial tumor. The resulting overlaps precluded diagnostic accuracy in the distinction of low- and high-grade tumors [22].

Conclusions

There is the substantial uptake of ^{13}N-ammonia in cerebral astrocytomas. ^{13}N-ammonia uptake in astrocytomas is related to the histological tumor grade, and ^{13}N-ammonia PET may enable differentiation between low- and high-grade astrocytomas, and has the potential to enable differentiation between low-grade astrocytomas and non-neoplastic lesions.

Acknowledgement

The authors are highly grateful to the anonymous referees for their significant and constructive critiques and suggestions, which improve the paper very much. This work was partially supported by grant 031652 from the Nature Sciences Foundation of Guangdong Province, China.

References

1. Ricci PE: Imaging of adult brain tumors. Neuroimag Clin N Am 9: 651–669, 1999
2. Chung JK, Kim YK, Kim SK et al.: Usefulness of ^{11}C-methionine PET in the evaluation of brain lesions that are hypo- or isometabolic on ^{18}F-FDG PET. Eur J Nucl Med 29: 176–182, 2002
3. Roelcke U, Radu EW, von Ammon K et al.: Alteration of blood–brain barrier in human brain tumors: comparison of [18F]fluorodeoxyglucose, [11C]methionine and rubidium-82 using PET. J Neurol Sci.132: 20–27, 1995
4. Ogawa T, Shishido F, Kanno I et al.: Cerebral glioma: evaluation with methionine PET. Radiology 186: 45–53, 1993
5. Ohtani T, Kurihara H, Ishiuch S et al.: Brain tumour imaging with ^{11}C-choline: comparison with FDG PET and gadolinium-enhanced MR imaging. Eur J Nucl Med 28: 1664–1679, 2001
6. Kleihues P, Cavenee W: Pathology and genetics of tumours of the nervous system. International Agency for Research on Cancer, Lyon, 2000, pp 107–109
7. Hoop B, Hnatowich DJ, Brownell GL et al.: Techniques for positron scintigraphy of the brain. J Nucl Med 17: 473–479, 1976
8. Schelstraete K, Simons M, Deman J et al.: Uptake of ^{13}N-ammonia by human tumours as studied by positron emission tomography. Br J Radiol 55: 797–804, 1982
9. Benard F, Romsa J, Hustinx R: Imaging gliomas with positron emission tomography and single-photon emission computed tomography. Semin Nucl Med 33: 148–162, 2003
10. Schelbert HR, Phelps ME, Huang SC et al.: N-13 ammonia as an indicator of myocardial blood flow. Circulation 63: 1259–1272, 1981
11. Phelps ME, Hoffman EJ, Coleman RE et al.: Tomographic images of blood pool and perfusion in brain and heart. J Nucl Med 17: 603–612, 1976
12. Phelps ME, Huang SC, Hoffman EJ et al.: Cerebral extraction of N-13 ammonia: its dependence on cerebral blood flow and capillary permeability-surface area product. Stroke 12: 607–619, 1981
13. Bergmann SR, Hack S, Tewson T et al.: The dependence of accumulation of $^{13}NH_3$ by myocardium on metabolic factors and its implications for quantitative assessment of perfusion. Circulation 61: 34–43, 1980
14. Cooper AJL, McDonald JM, Gelbard AS et al.: The metabolic fate of ^{13}N-labeled ammonia in rat brain. J Biol Chem 254: 4982–4992, 1979
15. Pilkington GJ, Lantos PL: The role of glutamine synthetase in the diagnosis of cerebral tumours. Neuropathol Appl Neurobiol 8: 227–236, 1982
16. Akimoto J: Immunohistochemical study of glutamine synthetase expression in normal human brain and intracranial tumors. No To Shinkei 45: 362–368, 1993
17. McCormick D, McQuaid S, McCusker et al.: A study of glutamine synthetase in normal human brain and intracranial tumours. Neuropathol Appl Neurobiol 16: 205–211, 1990
18. Mineura K, Sasajima T, Kowada M et al.: Perfusion and metabolism in predicting the survival of patients with cerebral gliomas. Cancer 73: 2386–2394, 1994
19. Pruel MC, Caramanos Z, Collins DL et al.: Accurate noninvasive diagnosis of human brain tumors by using proton magnetic resonance spectroscopy. Nature Med 2: 323–325, 1996
20. Somorjai RL, Dolenko B, Nikulin AK et al.: Classification of H MR spectra of human brain neoplasms: the influence of preprocessing and computerized consensus diagnosis classification accuracy. J Magn Reson Imaging 6: 437–444, 1996
21. Taylor JS, Langston JW, Peddick WE et al.: Clinical value of proton magnetic resonance spectroscopy for differentiating recurrent or residual brain tumor from delayed cerebral necrosis. Int J Radiat Oncol Biol Phys 36: 1251–1261, 1996
22. Negendank WG, Sauter R, Brown TR et al.: Proton magnetic resonance spectroscopy in patients with glial tumors: a multicenter study. J Neurosurg 84: 449–458, 1996

Address for offprints: Zhang Xiangsong, Department of Nuclear Medicine, The First Affiliated Hospital, Sun Yat-sen University, 58 Zhongshan Road II, 510089, Guangzhou, China; Tel.: +86-20-85582776; Fax: +86-20-87750632; E-mail: sd_zh@163.net